AJChE 2015, Vol. 15, No. 2, 33 – 50

Prediction of Density of Binary Mixtures of Ionic Liquids with Alcohols (Methanol/Ethanol/1-Propanol) using Artificial Neural Network

Karen Faith P. Ornedo - Ramos [1]
Carla Angela M. Muriel [1]
Adonis P. Adornado [1]
Allan N. Soriano [1]
Vergel C. Bungay [*, 2]
[1] *School of Chemical Engineering and Chemistry, Mapúa Institute of Technology, Manila*
[2] *Chemical Engineering Department, De La Salle University, Manila*
[*]*e-mail:* vergel.bungay@dlsu.edu.ph

Ionic liquids demonstrated successful potential applications in the industry most specifically as the new generation of solvents for catalysis and synthesis in chemical processes, thus knowledge of their physico-chemical properties is of great advantage. The present work presents a mathematical correlation that predicts density of binary mixtures of ionic liquids with various alcohols (ethanol/methanol/1-propanol). The artificial neural network algorithm was used to predict these properties based on the variations in temperature, mole fraction, number of carbon atoms in the cation, number of atoms in the anion, number of hydrogen atoms in the anion and number of carbon atoms in the alcohol. The data used for the calculations were taken from ILThermo Database. Total experimental data points of 1946 for the considered binaries were used to train the algorithm and to test the network obtained. The best neural network architecture determined was found to be 6-6-10-1 with a mean absolute error of 48.74 kg/m^3. The resulting correlation satisfactorily represents the considered binary systems and can be used accurately for solvent related calculations requiring properties of these systems.

Keywords: artificial neural network; ionic liquid; density; ethanol; methanol; propanol

INTRODUCTION

Ionic liquids (ILs) play a significant role in the development of industrial chemistry and chemical technology as novel solvents which belong to the class of molten salts at room temperature (Gardas and Coutinho, 2009). ILs exhibit desirable properties such as negligible vapor pressure, non-flammability, large range of densities and viscosities, high potential for recycling, and highly solvating capacity for

organic, inorganic and organometallic compounds. They are commonly known as the "green solvents" in industrial applications. The knowledge of viscosity, density and refractive index of aqueous ionic liquids solutions at various temperatures are required in both physical chemistry and chemical engineering calculations involving fluid flow, heat and mass transfer (Giro et al., 2003).

Diverse researches have been conducted for the potential applications of these ILs. They became significant solvents for chemical synthesis and catalysis, gas–liquid absorption, liquid membrane separations, fuel and solar cells, nanomaterial technologies, preparation of polymer-gel catalytic membranes and generation of high conductivity materials (Gardas and Coutinho, 2008). Such applications lead to the development of thermodynamic models for computing the thermo-physical properties of ionic liquids like COSMO-RS which are now widely-used and efficient tools for the prediction of properties of ionic liquids (Diedenhofen and Klamt, 2010). As assessed by the previous studies, prediction of physical properties can be made possible by varying only one or two parameters such as temperature and pressure, disregarding the effect of each composition of the compounds in the binary system (Liu et al., 2008). Hydroxyl ammonium ionic liquids mixed with organic solvents boost its absorption capacity for CO_2. In actual use, physico – chemical properties of hydroxyl ammonium ionic liquids with organic solvent mixtures are extremely important. Density and viscosity contributes of great importance in both practical and theoretical viewpoint. Although applications of ionic liquids are well known, detailed knowledge regarding the thermodynamic behavior of mixtures of ionic liquids with organic solvents has not received particularly large share of the literature on ionic liquid studies and is still limited (Kurnia et al., 2010).

A need for further development of these studies must be made to develop more accurate and efficient thermodynamic modeling in computing such properties, in conjunction with the fast growing number of binary ionic liquids with organic solvents. Predictive computing is one way of evaluating these thermo-physical properties and be able to generate model that predicts such physical property of binary ionic liquid solutions from various sources of data which were generally acquired from previous experiments through the use of some algorithm such as Artificial Neural Network (ANN). The ANN algorithm has been used for several applications, e.g. electronics, financial institutions, etc. but limited use of such algorithm has been made for chemical engineering applications.

The study aimed to develop a specific model that predicts the physical property, i.e., density of binary ionic liquid solutions containing methanol, ethanol, and 1-propanol. Specifically, it aimed to optimize the best neural architecture for ANN computation; to determine the empirical parameters for the optimized ANN model; and to predict the density from the obtained parameters.

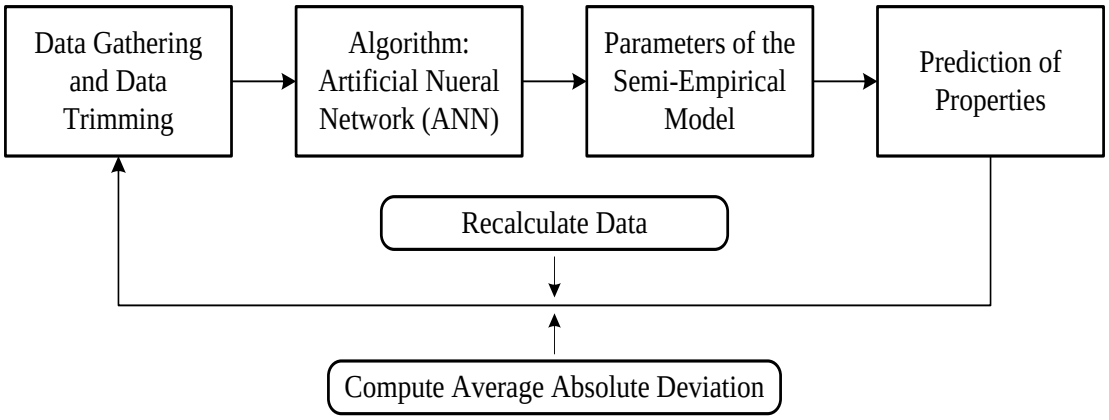

Fig. 1: Conceptual Framework

METHODS

Figure 1 presented the overall flow of process for the prediction of the considered properties. The details of each step were briefly discussed as follows:

Data gathering and data trimming

The present study is purely computational and the experimental data used for the calculations were taken from NIST Database, ILThermo. The complete details of the studied ionic liquids are included in the Appendix. A total of 6144 experimental data points for density were gathered. Tables 1 to 3 presented the details of these data, including the temperature range, pressure, mole fraction range, number of data points and the references for the respective binaries. Other information such as the number of atoms in the cation, number of CH_3R in the cation, number of atoms in the anion and number of hydrogen atoms in the anion of the ILs was also collected.

All the data gathered were initially assessed by observing the corresponding trends, and then removing the data that seems to disagree with the overall trend. Accurate and reliable data results were considered. Data trimming was done by graphing all the data gathered from different references. Graphs of temperature versus property and mole fraction versus property were plotted. These graphs formed smooth curves. Points that were observed to be far or out from the smooth curve were omitted or were trimmed. The trimmed data were compiled into one spread sheet in preparation for the utilization of the algorithm. For density calculations, the number of data points left after trimming was 1946. The detailed trimming process applied in the present study was adopted from previous works (Soriano *et al*., 2010; 2014).

Artificial neural network (ANN) algorithm

The ANN model used for the algorithm is shown in Figure 2, which includes one

Table 1. Density data for IL (1) + methanol (2) systems

IL Code	Temperature range (K)	Pressure (kPa)	Mole fraction range	Data points	Reference
C1A1	298.15-313.15	101.325	0-1.0	33	Deenadayalu and Bhujrajh, 2008
C1A6	298.15-328.15	101.325	0-1.0	39	Gonzalez *et al.*, 2007
	283.15-333.15	100-35000	0.06025-0.9522	693	Hofman *et al.*, 2008
C1A14	278.15-318.15	101.325	0.0511-0.9495	65	Vercher *et al.*, 2007
C2A8	298.15	101.325	0.0802-0.934	10	Domanska *et al.*, 2006
	313.15-333.15	100-25000	0.1212-0.9405	315	Goldon *et al.*, 2007
C4A2	298.15-313.15	101.325	0.055-0.979	48	Bhujrajh and Deenadayalu, 2007
C4A4	298.15-318.15	101.325	0.00151-0.1109	55	Zafarani-Moattar and Shekaari, 2006b
C4A5	293.15-318.15	101.325	0-0.518	60	Yang *et al.*, 2010
C4A7	298.15-318.15	101.325	0-1.0	60	Zafarani-Moattar and Shekaari, 2005b
	298.15	101.325	0.000426-0.0193	12	Zafarani-Moattar and Shekaari, 2006a
	298.15-398.15	101.325	0-1.0	360	Abdulagatov *et al.*, 2008b
C4A8	298.15	101.325	0.0692-0.9493	10	Domanska *et al.*, 2006
C4A10	298.15	101.325	0.092-0.9912	10	Domanska *et al.*, 2006
	298.15-298.15	290-40080	0-0.9662	315	Abdulagatov *et al.*, 2009
C4A12	298.15-318.15	101.325	0-1.0	50	Zafarani-Moattar and Shekaari, 2006b
	293.15-323.15	101.325	0-1.0	112	Iglesias-Otero *et al.*, 2007
	298.15-398.15	101.325	0.0898-0.9913	315	Abdulagatov *et al.*, 2008b
	298.15	101.325	0.00065-0.0202	12	Shekaari and Zafarani-Moattar, 2008
	298.15	101.325	0.4417-0.9926	11	Stoppa *et al.*, 2009
C4A13	298.15-328.15	101.325	0-1.0	52	Domanska and Laskowska, 2009
C5A12	298.15-323.15	101.325	0-1.0	39	Heintz *et al.*, 2002
	298.15-318.15	101.325	0.0954-0.9461	29	Ortega *et al.*, 2008
C7A2	298.15-315.15	101.325	0.110-0.909	18	Bhujrajh *et al.*, 2007
C7A3	298.15	101.325	0.0654-0.9020	10	Andreatta *et al.*, 2009b
C7A5	298.15-328.15	101.325	0-1.0	45	Gonzalez *et al.*, 2006
C7A12	298.15	101.325	0.0951-0.9505	13	Arce *et al.*, 2006a
Total No. of Data Points				2791	

input layer followed by hidden layer/s and an output layer being the last layer. The nodes in every layer were connected by weights ($w_{I'-n}$, $w_{n-n'}$ or $w_{n'-Y}$) as well as bias weights (w_{b-n}, $w_{b-n'}$ or w_{b-Y}) where the first subscript represents the source node and the second subscript represents the destination node.

In this study, aside from the temperature (*T*) and mole fraction of the IL (*X*), structure-related parameters such as number of carbon atoms in the cation (*NCC*), number of atoms in the anion (*NA*), number of hydrogen atoms in the anion (*NH*) and number of carbon atoms in the alcohol (*NCA*) were also considered in the input layer as suggested by Viswanadhan et al. (1989) and Valderama et al. (2010). To simplify the model, a maximum number of two hidden layers and a maximum of 10 nodes per hidden layer were imposed and that there is only one expected output per neural network architecture, i.e., the density.

Determination of the parameters of the model

The mean absolute error (lowest), MAE (Eq. 1) was assigned as the basis for determining the best neural network

Table 2. Density data for IL (1) + ethanol (2) systems

IL (1)	Temperature range (K)	Pressure (KPa)	Mole fraction range	Data points	References
C1A6	298.15-328.15	101.325	0-1.0	36	Gomez *et al.,* 2006b
	298.15	101	0.1271-0.9522	26	Arce *et al.,* 2006b
	293.15-318.15	101.325	0.0612-0.9843	84	Garcia-Miaja *et al.,* 2008
	283.15-343.15	100-35000	0.06825-0.94944	864	Matkowska *et al.,* 2010
C1A12	298.15	101.325	0-1.0	6	Rilo *et al.,* 2009
C1A14	278.15-328.15	101.325	0.0508-0.9501	78	Vercher *et al.,* 2007
	293.15-318.15	101.325	0.1216-0.9477	60	Garcia-Miaja *et al.,* 2008
C2A8	298.15	101.325	0.0449-0.9489	11	Domanska *et al.,* 2006
	293.15-303.15	101.325	0-1.0	39	Pereiro and Rodriguez, 2007
	298.15-328.15	100	0-1.0	39	Gomez *et al.,* 2008
C3A6	298.15-328.15	101.325	0-1.0	33	Gonzales *et al.,* 2009
C4A3	298.15	101.325	0.0793-0.8984	12	Andreatta *et al.,* 2010
C4A4	298.15-318.15	101.325	0.00125-0.01436	35	Zafarani-Moattar and Shekaari, 2005a
C4A5	298.15	101.325	0.1874-1.0	9	Calvar *et al.,* 2006
C4A7	293.15-303.15	101.325	0-1.0	39	Pereiro and Rodriguez, 2007
	298.15	101.325	0.0386-0.9287	10	Domanska *et al.,* 2006
	293.15-303.15	101.325	0-1.0	39	Pereiro and Rodriguez, 2007
	293.15-323.15	101.325	0-1.0	64	Iglesias-Otero *et al.,* 2008b
	298.15	101.325	0.0752-0.9541	14	Iglesias-Otero *et al.,* 2008a
	293.15-318.15	101.325	0.0632-0.9489	66	Garcia-Miaja *et al.,* 2008
	298.15-328.15	100	0-1.0	39	Gonzalez *et al.,* 2008
C4A9	283.15-333.15	101.325	0.110-0.852	88	Mokhtarani *et al.,* 2009
C4A11	283.15-313.15	101.325	0.1-0.860	71	Mokhtarani *et al.,* 2008
C4A12	293.15-323.15	101.325	0-1.0	56	Iglesias-Otero *et al.,* 2008b
	298.15-398.15	390-39560	0-0.9299	270	Abdulagatov *et al.,* 2008a
	298.15	101.325	0.1705-0.9483	11	Iglesias-Otero *et al.,* 2008a
	293.15-318.15	101.325	0.1179-0.9013	54	Garcia-Miaja *et al.,* 2008
	313.15-433.15	200-2000	0-1.0	200	Han *et al.,* 2009
	298.15	101.325	0-0.9014	13	Rilo *et al.,* 2009
C4A13	298.15-348.15	101.325	0-1.0	65	Domanska and Laskowska, 2009
C4A14	293.15-318.15	101.325	0.0717-0.9478	66	Garcia-Miaja et al., 2008
C5A12	298.15-318.15	101.325	0.1224-0.9477	28	Ortega et al., 2008
C6A5	298.15	101.325	0-1.0	12	Gomez et al., 2006a
C6A7	293.15-303.15	101.325	0-1.0	40	Pereiro and Rodriguez, 2007
C6A12	293.15-318.15	101.325	0.1479-0.8948	60	Garcia-Miaja et al., 2008
	298.15	101.325	0-0.902	10	Rilo et al., 2009
C7A3	298.15	101.325	0.0959-0.8967	11	Andreatta et al., 2009a
C7A5	298.15-328.15	101.325	0-1.0	33	Gonzalez et al., 2006
C7A7	293.15-303.15	101.325	0-1.0	39	Pereiro and Rodriguez, 2007
C7A12	298.15	101.325	0.0714-0.9483	13	Arce et al., 2006b
	283.15-343.15	101.325	0.081-0.753	78	Mokhtarani et al., 2008
	298.15	101.325	0-0.8988	10	Rilo et al., 2009
Total No. of Data Points				2831	

architecture. In Eq. (1), L is the total number of data points, Y_l is the predicted value and E_l is the experimental or actual value. The flowchart for choosing the best neural network architecture is shown in Figure 3.

$$MAE = \frac{1}{L}\sum_{l=1}^{L}\left|Y_l - E_l\right| \quad (1)$$

Table 3. Density data for IL (1) + 1-propanol (2) systems

IL Code	Temperature range (K)	Pressure (kPa)	Mole fraction range	Data points	Reference
C1A6	298.15-328.15	101.325	0-1.0	33	Gonzalez et al., 2007
	298.15	101.325	0-1.0	14	Domanska and Laskowska, 2008
C1A14	278.15-338.15	101.325	0.049-0.9499	91	Vercher et al., 2007
C3A6	298.15-328.15	101.325	0-1.0	36	Gonzalez et al., 2009
C4A3	298	101.325	0-1.0	11	Wandschneider et al., 2008
C4A9	293.15-333.15	101.325	0.121-0.857	88	Mokhtarani et al., 2009
C4A10	278.15-318.15	101.325	0-0.07277	30	Orchilles et al., 2006
C4A12	293.15	101.325	0-1.0	72	Huo et al., 2007
C4A13	298.15-348.15	101.325	0-1.0	72	Domanska et al., 2009
C5A12	298.15-318.15	101.325	0.0809-0.9846	23	Ortega et al., 2008
C7A5	298.15-328.15	101.325	0-1.0	39	Gonzalez et al., 2006
C7A12	298.15	101.325	0.0082-0.9527	13	Arce et al., 2006a
Total No. of Data Points				2791	

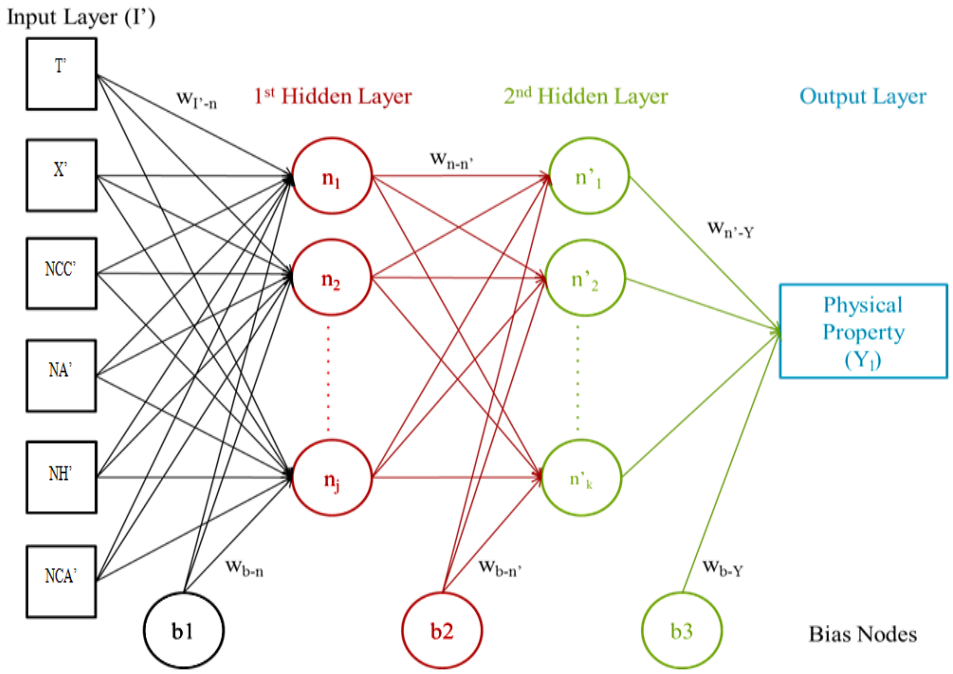

Fig. 2: ANN model with two hidden layers

The mathematical relationship between inputs, hidden layers and outputs is described by weights, bias weights, and transfer functions (Nguyen et al., 2007):

$$n_j = f\left[\sum_{j=1}^{J}(I')(w_{l-n}+1)(w_{b-n})\right] \quad (2)$$

$$n'_k = f\left[\sum_{k=1}^{K'}(n_j)(w_{n-n'}+1)(w_{b-n'})\right] \quad (3)$$

$$Y'_l = f\left[\sum_{l=1}^{L'}(n'_k)(w_{n'-Y}+1)(w_{b-Y})\right] \quad (4)$$

The transfer function used:

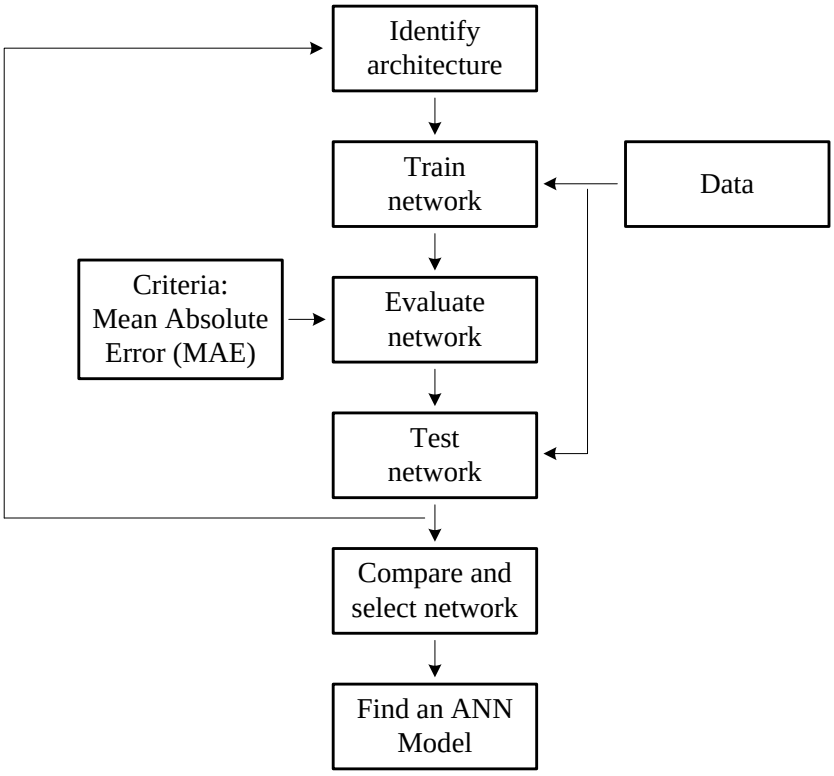

Fig. 3: Flowchart for determining neural network architecture

$$f_1 = \log sig = \frac{1}{1+e^{-x}} \quad (5)$$

The *I'* in Eq. (2) is a function of the input variables: *T, X, NCC, NA, NH,* and *NCA* and its corresponding slope, m_i and intercept, b_i and can be expressed as:

$$I' = m_i I + b_i \quad (6)$$

The three termination criteria for training of ANN are the maximum number of epochs, training time and target mean square error, MSE (Eq. 7).

$$\mathrm{MSE} = \frac{1}{L}\sum_{l=1}^{L}\left(Y_l - E_l\right)^2 \quad (7)$$

In the calculations, ninety percent (90%) of the experimental data was used in training the neural network and remaining ten percent (10%) of data was used in testing the generated model. After the training process, the parameters were obtained and the best neural network architecture was chosen.

Prediction of properties

All data points for density were re-calculated using Eq. (9) where Y_l is the predicted value and Y_l' is the output node and is a function of the determined weights, bias weights and the corresponding slope and intercept for the given set of data points (Eq. 4).

$$Y'_l = m_l Y_l + b_l \quad (8)$$

$$Y_l = \frac{Y'_l - b_l}{m_l} \quad (9)$$

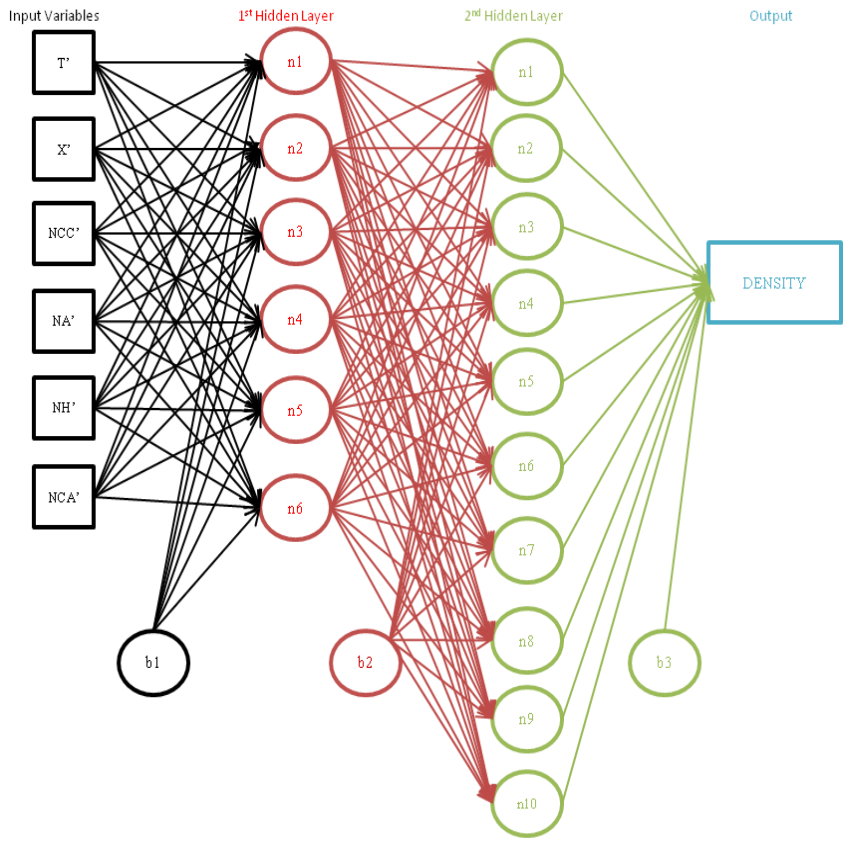

Fig. 4: Best neural network architecture for density calculations.

Finally, the mean absolute error was determined using Eq. (1). For the purpose of interpreting the result, the percentage error, as in Eq. (10) was also determined and the predicted and experimental values of the properties were classified and plotted based on the percentage error. Percentage error ranging from 0-1% was marked green, 1-5% was marked yellow and error more than 5% was marked red.

$$\text{Percentage error} = \frac{|E_l - Y_l|}{E_l} \times 100\% \qquad (10)$$

RESULTS AND DISCUSSION

There were 6144 data points collected for density which were obtained from various literatures as summarized by the ILThermo Database. Out of the total data points, only 1946 trimmed binary IL data were used for the calculations, i.e., training the network and obtaining the optimum neural network parameters. These parameters were adjusted for different trial-and-error stage (epoch) until the best neural network architecture was determined.

Figure 4 shows the best neural network architecture in predicting density. This model is called 6-6-5-1 neural network architecture. This network architecture means that each weight from the input layer is being sent to the 6 nodes of the first hidden layer. Then each weight from the first hidden layer goes to the five nodes of the second hidden layer. The weights produced from the second hidden

Table 4. Prediction of density of the considered IL (1) + methanol (2) systems

IL Code	Temperature Range (K)	Mole Fraction Range	Experimental Density Range (kg/m^3)	% Error	No. of Data Points
C1A1	298.15-313.15	0.0000-1.0000	799.1-1391.0	10.28%	12
C1A6	283.15-328.15	0.0000-1.0000	814.4-1200.3	4.07%	108
C1A8	298.15-333.15	0.0595-0.8788	888.2-1256.0	3.91%	50
C4A2	298.15-313.15	0.055-0.9790	808.8-1101.5	9.49%	48
C4A4	298.15-318.15	0.00151-0.1109	846.5-953.0	5.77%	55
C4A5	293.15-318.15	0.0000-0.5180	845.1-1054.8	6.05%	60
C4A8	298.15	0.0692-0.9493	875.0-1093.6	7.11%	10
C4A13	298.15-328.15	0.0000-1.0000	828.2-1106.5	4.89%	52
C7A2	298.15-315.15	0.110-0.9090	858.3-1042.4	7.05%	18
C7A3	298.15	0.0654-0.9020	869.0-1070.0	18.33%	10
C7A5	298.15-328.15	0.0000-1.0000	840.8-1072.3	7.76%	45
C7A12	298.15	0.0951-0.9505	883.2-1066.8	1.84%	13
		Total		6.04%	481

Table 5. Prediction of density of the considered IL (1) + ethanol (2) systems

IL Code	Temperature Range (K)	Mole Fraction Range	Experimental Density Range (kg/m^3)	% Error	No. of Data Points
C1A6	283.15-343.15	0.0000-1.0000	800.7-1256.7	4.85%	241
C1A8	293.15-328.15	0.0000-1.0000	821.5-1281.7	4.05%	84
C1A12	298.15	0.0714-0.9483	881.3-1330.4	13.50%	13
C1A14	278.15-328.15	0.0508-0.9501	844.7-1247.8	3.78%	138
C3A6	298.15-328.15	0.0000-1.0000	808.7-1153.2	4.72%	33
C4A3	298.15	0.0793-0.8984	914.7-1242.5	9.62%	7
C4A4	298.15-318.15	0.0013-0.0144	838.2-864.3	8.00%	35
C4A5	298.15	0.1874-1.0000	851.4-1080.4	6.34%	9
C4A9	283.15-333.15	0.1100-0.8520	944.6-1105.0	2.75%	88
C4A11	283.15-313.15	0.1000-0.8600	944.8-1094.5	6.71%	45
C4A13	298.15-348.15	0.0000-1.0000	809.3-1117.1	6.98%	65
C6A5	298.15	0.0000-1.0000	854.7-1373.6	3.27%	6
C6A7	293.15-303.15	0.0000-1.0000	823.3-1213.2	3.74%	40
C6A12	293.15-318.15	0.0000-0.9020	908.5-1079.4	2.87%	70
C7A3	298.15	0.0959-0.8967	865.5-1068.7	6.12%	11
C7A5	298.15-328.15	0.0000-1.0000	833.0-1072.5	8.66%	33
C7A7	293.15-303.15	0.0000-1.0000	819.5-1071.7	9.03%	39
		Total		5.18%	957

layer are called the output weights. The bias weights and the output bias weight also went to every node in the hidden layer. This best neural network architecture resulted to mean absolute error of 48.74 kg/m^3, having an average percentage error of 4.46 %, as specifically presented in Tables 4 to 6.

Table 6. Prediction of density of the considered IL (1) + 1-propanol (2) systems

IL Code	Temperature Range (K)	Mole Fraction Range	Experimental Density Range (kg/m^3)	% Error	No. of Data Points
C1A6	298.15-328.15	0.0000-1.0000	791.0-1290.6	2.91%	38
C1A14	278.15-338.15	0.0490-0.9499	830.9-1382.6	1.32%	91
C3A6	298.15-328.15	0.0000-1.0000	788.4-1234.5	0.99%	36
C4A3	298	0.0000-1.0000	802.5-1226.5	3.33%	6
C4A9	293.15-333.15	0.1210-0.8570	882.1-1166.6	1.78%	88
C4A10	278.15-318.15	0.0000-0.0728	796.8-913.4	1.19%	30
C4A12	293.15	0.0000-1.0000	780.5-1173.0	1.46%	72
C4A13	298.15-348.15	0.0000-1.0000	776.7-1135.2	3.51%	72
C5A12	298.15-318.15	0.0809-0.9846	821.5-1158.3	0.76%	23
C7A5	298.15-328.15	0.0000-1.0000	782.6-1029.1	1.46%	39
C7A12	298.15	0.0082-0.9527	853.0-1144.7	4.62%	13
		Total		6.04%	481

The percentage errors for the prediction of density were ranging from (1.84–18.33 %), (2.75–13.50 %), and (0.76–4.62 %) for binary IL system with methanol, ethanol, and 1-propanol, as presented in Tables 4,5 and 6, respectively. The calculation results showed that the binary system consisting of 1-methyl-3-octylimidazolium bis [(trifluoromethyl) sulfonyl] imide (C7A3) and methanol with 10 data points led to the highest percentage error and the binary system of 1 – butyl – 4 – methylpyridinium tetrafluoroborate (C5A12) and 1-propanol having 23 data points has the lowest percentage error acquired. Such high percentage errors could be attributed to the inconsistency of experimental data which might be due to impurities of the substances or the inaccuracy of the instruments and measurement methods. Overall, the calculated percentage errors for density led to a good prediction as shown by an overall percentage error of 4.46 % for a total of 1946 data points.

Tables 7 to 9 show the values of the weights and bias weights that resulted from applying the ANN algorithm in the prediction of density. These values are the result of the density property modeling which obtained the following best neural network architecture for the three alcohols which is 6-6-10-1. The simplified generated equation for the prediction of density is given in Eq. (11) which is a function of parameters A, $B_{n'}$ and C_n. Here, the parameter C_n is a function of T, X, NCC, NA, NH, and NCA.

$$\text{Predicted density} = \frac{1}{0.0012}\left(\frac{1}{1+e^{-A}}\right) - 722.333 \quad (11)$$

$$A = \sum_{n'=1}^{5}\left[W_{b-Y} + W_{n'-Y}\left(\frac{1}{1+e^{-B_{n'}}}\right)\right] \quad (11\text{-a})$$

$$B_{n'} = \sum_{n=1}^{6}\left[W_{b-n'} + W_{n-n'}\left(\frac{1}{1+e^{-C_n}}\right)\right] \quad (11\text{-b})$$

Table 7. Weights and bias weight for hidden layer 1

N	$w_{b\text{-}n}$	$w_{T\text{-}n}$	$w_{X\text{-}n}$	$w_{NCC\text{-}n}$	$w_{NA\text{-}n}$	$w_{NH\text{-}n}$	$w_{NCA\text{-}n}$
1	0.7280	-0.4674	-0.8391	-0.4261	5.5493	-5.1527	0.3429
2	-0.3413	-0.3135	-0.4731	-0.0355	0.1239	0.0522	-0.6640
3	0.7225	0.2206	-3.2701	-1.0472	-1.1601	-1.6074	1.1342
4	2.6039	-0.7382	-1.3733	4.5201	-3.7763	2.8212	-0.1222
5	-1.2158	0.6865	-10.8440	-0.1471	2.0057	-1.3101	0.2185
6	-0.0015	-0.0328	-2.2341	0.1008	0.6625	0.8402	-0.0106

Table 8. Weights and bias weight for hidden layer 2

n'	$w_{b\text{-}n'}$	$w_{1\text{-}n'}$	$w_{2\text{-}n'}$	$w_{3\text{-}n'}$	$w_{4\text{-}n'}$	$w_{5\text{-}n'}$	$w_{6\text{-}n'}$
1′	-0.3911	0.0574	-0.0163	-0.0936	-0.2325	-0.1208	0.2883
2′	0.0983	0.9683	0.1982	-0.8596	-1.4788	-1.8013	-0.2031
3′	-0.1527	0.5795	-0.4707	-0.2379	-1.0287	-0.8437	-0.7145
4′	0.3239	0.9920	-0.2450	-0.7687	-0.4106	-1.6264	-0.5324
5′	-0.0699	-0.8325	0.3289	0.6523	0.5428	0.9378	0.1908
6′	-0.4978	-1.3258	-0.1224	0.4315	0.5872	1.7996	0.4355
7′	-0.4388	0.2391	0.1011	-0.2718	-0.5748	-0.1875	0.0062
8′	-0.4745	-1.1745	-0.2377	0.5768	0.7125	1.5954	-0.2249
9′	-0.2672	-0.6156	0.2156	-0.0443	0.0146	1.2225	0.3799
10′	-0.4644	-0.1972	-0.3677	0.3961	0.2437	-0.3796	-0.1892

Table 9. Weights and bias weight for the output layer

$w_{b\text{-}Y}$	$w_{1'\text{-}Y}$	$w_{2'\text{-}Y}$	$w_{3'\text{-}Y}$	$w_{4'\text{-}Y}$	$w_{5'\text{-}Y}$
0.1331	0.1169	2.5970	1.4678	2.0121	-1.5020

$w_{6'\text{-}Y}$	$w_{7'\text{-}Y}$	$w_{8'\text{-}Y}$	$w_{9'\text{-}Y}$	$w_{10'\text{-}Y}$
-2.2819	0.3867	-1.9859	-1.2140	-0.0058

$$C_n = w_{b-n} + 0.0143w_{T-n}(T - 277.87) + w_{x-n}X + 0.1429w_{NCC-n}(NCC - 5) + 0.0345w_{NA-n}(NA - 1) + 0.0588w_{NH-n}NH + 0.5w_{NCA-n}(NCA - 1) \quad (11\text{-c})$$

As shown in Figure 5, the best neural network architecture was able to predict the experimental values successfully where the predicted values of density were found to be in good agreement with the experimental data. Of the calculated density, 13.13 % were within the percentage error range of 0–1 % which was marked green in Figure 5, 51.21 % were in the range of 1–5 % which was marked yellow and 35.66 % of the studied compounds have the percentage error higher than 5 % which were marked red. Although the number of data points with

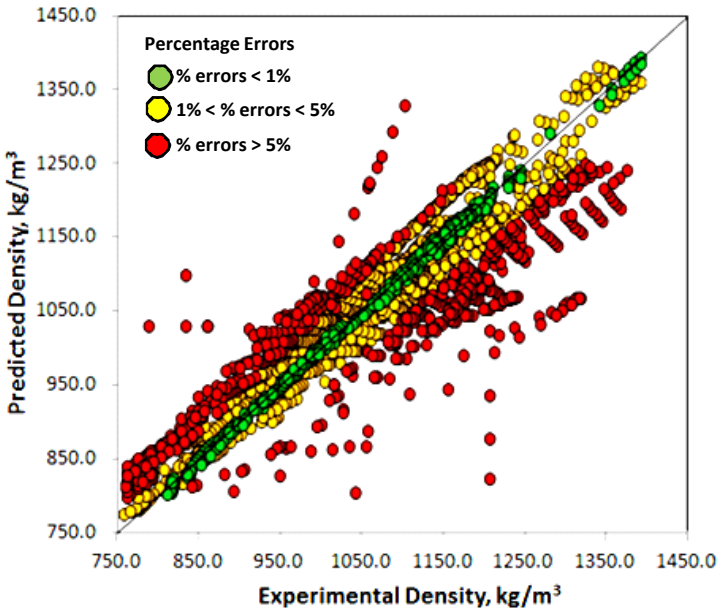

Fig.5: Predicted density versus experimental density

percentage error greater than 5 % is high but compared to the combined percentage of acceptable error which amounts to 64.34 %, the model obtained using the 6-6-10-1 architecture can be deemed as acceptable.

CONCLUSION

Artificial neural network (ANN) can be utilized as an algorithm in designing a model that will help predict the density of binary mixture of ionic liquid solutions with various alcohols such as: ethanol, methanol and 1-propanol. Density data from ILThermo Database was utilized and the densities were predicted as functions of temperature, mole fraction, number of carbon group in the cation, number of atoms in the anion, number of hydrogen atoms in anion and the number of carbon atoms in the alcohol. Using ANN, the best neural network architecture acquired has six nodes in the first hidden layer and ten nodes in the second hidden layer, having a mean absolute error of 48.74 kg/m^3 and an average percentage error of 4.46 %. Among the considered binaries containing IL (1) + Alcohol (2), the binary system containing 1-propanol shows the lowest percentage error of 1.91 % due to the consistency of the experimental data used for the modeling. Overall, there is a good agreement between the experimental density data with the predicted data using ANN. If no experimental data is available, the proposed model is a potential tool to estimate the density of binary ionic liquid solutions containing the alcohols methanol/ethanol/1-propanol.

APPENDIX

Cation Name	Structure	Cation Code
1-Ethyl-3-methylimidazolium	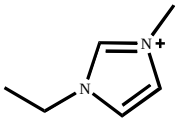	C1

Cation Name	Structure	Cation Code
1,3-Dimethylimidazolium	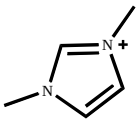	C2
1-Ethylpyridinium	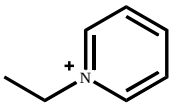	C3
1-Butyl-3-methylimidazolium	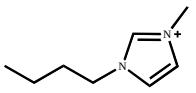	C4
1-Butyl-4-methylpyridinium	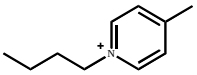	C5
1-Hexyl-3-methylimidazolium	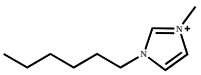	C6
1-Methyl-3-octylimidazolium	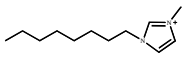	C7

Anion Name	Structure	Anion Code
1,1,2,2,2-Pentafluoro-n-[(pentafluoroethyl)sulfonyl] ethane-sulfonamide	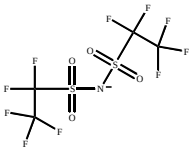	A1
2-(2-Methoxyethoxy)ethyl sulfate	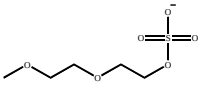	A2
Bis[(trifluoromethyl)sulfonyl] imide	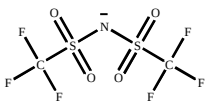	A3
Bromide	Br^-	A4

Anion Name	Structure	Anion Code
Chloride	Cl^-	A5
Ethylsulfate	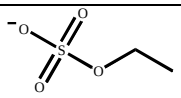	A6
Hexafluorophosphate	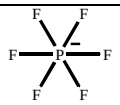	A7
Methyl sulfate	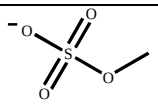	A8
Nitrate	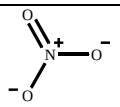	A9
Octylsulfate	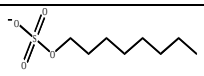	A10
Perchlorate	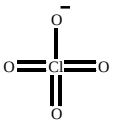	A11
Tetrafluoroborate	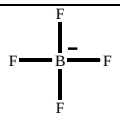	A12
Thiocyanate		A13
Trifluoromethanesulfonate	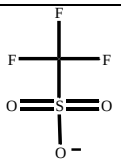	A14

REFERENCES

1. Abdulagatov, I. M., A. Tekin, J. Safarov, and E. Hassel (2008a). Densities and excess, apparent, and partial molar volumes of binary mixtures of $BMIMBF_4$ + ethanol as a function of temperature, pressure, and concentration. *Int. J. Thermophys.*, Vol. **29**, 505-533.
2. Abdulagatov, I. M., A. Tekin, J. Safarov, A. Shahverdiyev, and E. Hassel (2008b). High-pressure densities and derived volumetric properties (excess, apparent, and partial molar volumes)

of binary mixtures of {methanol (1) + [BMIM][BF_4] (2)}. *J. Chem. Thermodyn.*, Vol. **40**, 1386-1401.

3. Abdulagatov, I. M., J. Safarov, T. Guliyev, A. Shahverdiyev, and E. Hassel (2009). High temperature and high pressure volumetric properties of (methanolY[BMIMY][$OcSOZ_4$]) mixtures. *Phys. Chem. Liq.*, Vol. **47**, 9-34.
4. Andreatta, A. E., A. Arce, E. Rodil, and A. Soto (2009a). Physical properties of binary and ternary mixtures of ethyl acetate, ethanol, and 1-octyl-3-methyl-imidazolium bis(trifluoromethylsulfonyl)imide at 298.15 K. *J. Chem. Eng. Data*, Vol. **54**, 1022.
5. Andreatta, A. E., A. Arce, E. Rodil, and A. Soto (2009b). Physical and excess properties of (methyl acetate + methanol + 1-octyl-3-methyl-imidazolium bis(trifluoromethylsulfonyl)imide) and its binary mixtures at *T* = 298.15 K and atmospheric pressure. *J. Chem. Thermodyn.*, Vol. **41**, 1317-1323.
6. Andreatta, A. E., A. Arce, E. Rodil, and A. Soto (2010). Physico-chemical properties of binary and ternary mixtures of ethyl acetate + ethanol + 1-butyl-3-methyl-imidazolium bis(trifluoromethylsulfonyl)imide at 298.15 K and atmospheric pressure. *J. Solution Chem.*, Vol. **39**, 371-383.
7. Arce, A., H. Rodriguez, and A. Soto (2006a). Effect of anion fluorination in 1-ethyl-3-methylimidazolium as solvent for the liquid extraction of ethanol from ethyl tert-butyl ether. *Fluid Phase Equilib.*, Vol. **242**, 164-168.
8. Arce, A., E. Rodil, and A. Soto (2006b). Volumetric and viscosity study for the mixtures of 2-ethoxy-2-methylpropane, ethanol, and 1-ethyl-3-methylimidazolium ethyl sulfate ionic liquid. *J. Chem. Eng. Data*, Vol. **51**, 1453-1457.
9. Bhujrajh, P. and N. Deenadayalu (2007). Liquid densities and excess molar volumes for binary systems (ionic liquids + methanol or water) at 298.15, 303.15 and 313.15 K, and at atmospheric pressure. *J. Solution Chem.*, Vol. **36**, 631-642.
10. Calvar, N., B. Gonzales, E. Gomez, and A. Dominguez (2006). Vapor-liquid equilibria for the ternary system ethanol + water + 1-butyl-3-methylimidazolium chloride and the corresponding binary systems at 101.3 kPa. *J. Chem. Eng. Data*, Vol. **51**, 2178-2181.
11. Deenadayalu, N. and P. Bhujrajh (2008). Density, speed of sound, and derived thermodynamic properties of ionic liquids [EMIM]+[BETI]- or ([EMIM]+[$CH_3(OCH_2CH_2)_2OSO_3$]- + methanol or + acetone) at *T* = (298.15 or 303.15 or 313.15) K. *J. Chem. Eng. Data*, Vol. **53**, 1098-1102.
12. Diedenhofen, M. and A. Klamt (2010). COSMO-RS as a tool for property prediction of IL mixtures- A review**.** *Fluid Phase Equilib.,* Vol. **294**, 31-38.
13. Domanska, U., A. Pobudkowska, and A. Wisniewska (2006). Solubility and excess molar properties of 1,3-dimethylimidazolium methylsulfate, or 1-butyl-3-methylimidazolium methylsulfate, or 1-butyl-3-methylimidazolium octylsulfate ionic

liquids with n-alkanes and alcohols: analysis in terms of the PFP and FBT models. *J. Solution Chem.*, Vol. **35**, 311-334.

14. Domanska, U. and M. Laskowska (2008). Phase equilibria and volumetric properties of (1-ethyl-3-methylimidazolium ethylsulfate + alcohol or water) binary systems. *J. Solution Chem.*, Vol. **37**, 1271-1287.
15. Domanska, U. and M. Laskowska (2009). Temperature and composition dependence of the density and viscosity of binary mixtures of {1-butyl-3-methylimidazolium thiocyanate + 1-alcohols}. *J. Chem. Eng. Data*, Vol. **54**, 2113-2119.
16. Garcia-Miaja, G., J. Troncoso, and L. Romani (2008). Excess properties for binary systems ionic liquid + ethanol: Experimental results and theoretical description using the ERAS model. *Fluid Phase Equilib.*, Vol. **274**, 59-67.
17. Gardas, R. L. and J. A. P. Coutinho (2008). A group contribution method for the viscosity estimation of ionic liquids. *Fluid Phase Equilib.,* Vol. **266**, 195-201.
18. Gardas, R. L. and J. A. P. Coutinho (2009). Group contribution methods for the prediction of thermophysical and transport properties of ionic liquids. *AIChE J.*, Vol. **55**, 1274-1290.
19. Giro, F. M., F. A. Gonzales, and A. G. M. Ferreira., I. M. A. Fonseca (2003). Viscosity and density data of the system water + n-pentyl acetate + methanol: calculations with a modified Redlich-Kwong-Soave equation of state. *Fluid Phase Equilib.,* Vol. **204**, 217.
20. Goldon, A., K. Dabrowska, and T. Hofman (2007). Densities and excess volumes of the 1,3-dimethylimidazolium methylsulfate + methanol system at temperatures from (313.15 to 333.15) K and pressures from (0.1 to 25) MPa. *J. Chem. Eng. Data*, Vol. **52**, 1830-1837.
21. Gomez, E., N. Calvar, I. Dominguez, and A. Dominguez (2006a). Physical properties of the ternary mixture ethanol + water + 1-hexyl-3-methylimidazolium chloride at 298.15K. *Phys. Chem. Liq.*, Vol. **44**, 409-417.
22. Gomez, E., B. Gonzalez, N. Calvar, E. Tojo, and A. Dominguez (2006b). Physical properties of pure 1-ethyl-3-methylimidazolium ethylsulfate and its binary mixtures with ethanol and water at several temperatures. *J. Chem. Eng. Data*, Vol. **51**, 2096-2102.
23. Gomez, E., B. Gonzalez, N. Calvar, and A. Dominguez (2008). Excess molar properties of ternary system (ethanol + water + 1,3-dimethylimidazolium methyl sulfate) and its binary mixtures at several temperatures. *J. Chem. Thermodyn.*, Vol. **40**, 1208-1216.
24. Gonzalez, E. J., L. Alonso, and A. Dominguez (2006). Physical properties of binary mixtures of the ionic liquid 1-methyl-3-octylimidazolium chloride with methanol, ethanol, and 1-propanol at T = (298.15, 313.15, and 328.15) K and at P) 0.1 MPa. *J. Chem. Eng. Data*, Vol. **51**, 1446-1452.
25. Gonzalez, E. J., B. Gonzales, N. Calvar, and A. Dominguez (2007). Physical properties of binary mixtures of the ionic liquid 1-ethyl-3-

methylimidazolium ethyl sulfate with several alcohols at *T* = (298.15, 313.15, and 328.15) K and atmospheric pressure. *J. Chem. Eng. Data*, Vol. **52**, 1641-1648.

26. Gonzalez, B., N. Calvar, E. Gomez, and A. Dominguez (2008). Physical properties of the ternary system (ethanol + water + 1-butyl-3-methylimidazolium methylsulphate) and its binary mixtures at several temperatures. *J. Chem. Thermodyn.*, Vol. **40**, 1274-1281.
27. Gonzalez, B., N. Calvar, E. Gomez, I. Dominguez, and A. Dominguez (2009). Synthesis and physical properties of 1-ethylpyridinium ethylsulfate and its binary mixtures with ethanol and 1-propanol at several temperatures. *J. Chem. Eng. Data*, Vol. **54**, 1353-1358.
28. Han, C., S. Xia, P. Ma, and F. Zeng (2009). Densities of ionic liquid [BMIM][BF_4] + ethanol, + benzene, and + acetonitrile at different temperature and pressure. *J. Chem. Eng. Data*, Vol. **54**, 2971-2977.
29. Heintz, A., D. Klasen, and J. K. Lehmann (2002). Excess molar volumes and viscosities of binary mixtures of methanol and the ionic liquid 4-methyl-n-butylpyridinium tetrafluoroborate at 25, 40, and 50 deg C. *J. Solution Chem.*, Vol. **31**, 467-476.
30. Hofman, T., A. Goldon, A. Nevines, and T. M. Letcher (2008). Densities, excess volumes, isobaric expansivity, and isothermal compressibility of the (1-ethyl-3-methylimidazolium ethylsulfate + methanol) system at temperatures (283.15 to 333.15) K and pressures from (0.1 to 35) MPa. *J. Chem. Thermodyn.*, Vol. **40**, 580-591.
31. Huo, Y., S. Xia, and P. Ma (2007). Densities of ionic liquids, 1-butyl-3-methylimidazolium hexafluorophosphate and 1-butyl-3-methylimidazolium tetrafluoroborate, with benzene, acetonitrile, and 1-propanol at *T* = (293.15 to 343.15) K. *J. Chem. Eng. Data*, Vol. **52**, 2077-2082.
32. Iglesias-Otero, M. A., J. Troncoso, and E. Carballo (2007). Density and refractive index for binary systems of the ionic liquid [Bmim][BF_4] with methanol, 1,3-dichloropropane, and dimethyl carbonate. *J. Solution Chem.*, Vol. **36**, 1219-1230.
33. Iglesias-Otero, M. A., J. Troncoso, E. Carballo, and L. Romani (2008a). Density and refractive index in mixtures of ionic liquids and organic solvents: Correlations and predictions. *J. Chem. Thermodyn.*, Vol. **40**, 949-956.
34. Iglesias-Otero, M. A., J. Troncoso, E. Carballo, and L. Romani (2008b). Densities and excess enthalpies for ionic liquids + ethanol or + nitromethane. *J. Chem. Eng. Data*, Vol. **53**, 1298-1301.
35. Kurnia, A., Wilfred, C.D, and T. Murugesan, 2009. Thermophysical properties of hydroxyl ammonium ionic liquids. *J. Chem. Thermodyn.*, Vol. **41**, 517-521.
36. Liu, W., L. Cheng, Y. Zhang, H. Wang, and M. Yu (2008). The physical properties of aqueous solution of room-temperature ionic liquids based on imidazolium: database and evaluation. *J. Mol. Liq.,* Vol. **140**, 68-72.
37. Matkowska, D., A. Golden, and T.Hofman (2010). Densities, excess

volumes, isobaric expansivities, and isothermal compressibilities of the 1-ethyl-3-methylimidazolium ethylsulfate + ethanol system at temperatures (283.15 to 343.15) K and pressures from (0.1 to 35) MPa. *J. Chem. Eng. Data*, Vol. **55**, 685-693.

38. Mokhtarani, B., M. M. Mojtahedi, H. R. Mortaheb, M. Mafi, F. Yazdani, and F. Sadeghian (2008). Densities, refractive indices, and viscosities of the ionic liquids 1-methyl-3-octylimidazolium tetrafluoroborate and 1-methyl-3-butylimidazolium perchlorate and their binary mixtures with ethanol at several temperatures. *J. Chem. Eng. Data*, Vol. **53**, 677-682.
39. Mokhtarani, B., A. Sharifi, H. R. Mortaheb, M. Mirzaei, M. Mafi, and F. Sadeghian (2009). Density and viscosity of 1-butyl-3-methylimidazolium nitrate with ethanol, 1-propanol, or 1-butanol at several temperatures. *J. Chem. Thermodyn.*, Vol. **41**, 1432-1438.
40. Orchilles, A. V., V. Gonzalez-Alfaro, P. J. Miguel, E. Vercher, and A. Martinez-Andreu (2006). Volumetric properties of binary mixtures of ionic liquid 1-butyl-3-methylimidazolium octylsulfate with water or propanol in the temperature range of 278.15 K to 328.15 K. *J. Chem. Thermodyn.*, Vol. **38**, 1124-1129.
41. Ortega. J., R. Vreekamp, E. Penco, and E. Marrero (2008). Mixing thermodynamic properties of 1-butyl-4-methylpyridinium tetrafluoroborate [$b_4$mpy][BF_4] with water and with an alkan-1ol (methanol to pentanol). *J. Chem. Thermodyn.*, Vol. **40**, 1087-1094.
42. Pereiro, A. B. and A. Rodriguez (2007). Study on the phase behaviour and thermodynamic properties of ionic liquids containing imidazolium cation with ethanol at several temperatures. *J. Chem. Thermodyn.*, Vol. **39**, 978-989.
43. Rilo, E., J. Pico, S. Garcia-Garabal, L. M. Varela, and O. Cabeza (2009). Density and surface tension in binary mixtures of CnMIM-BF_4 ionic liquids with water and ethanol. *Fluid Phase Equilib.*, Vol. **285**, 83-89.
44. Shekaari, H. and M. T. Zafarani-Moattar (2008). Volumetric properties of the ionic liquid, 1-butyl-3-methylimidazolium tetrafluoroborate, in organic solvents at T = 298.15 K. *Int. J. Thermophys.*, Vol. **29**, 534-545.
45. Soriano, A. N., A. Agapito, L. J. L. Lagumbay, A. R. Caparanga, and M-H.Li (2010).A simple approach to predict molar heat capacity of ionic liquids using group-additivity method. *J. Taiwan Inst. Chem. Engrs.*, Vol. **41**, 307-314.
46. Soriano A. N., M. K. L. Gimena, R. R. C. Rivera, M. A. M. Garcia, and R. R. Tan, (2014). Prediction of density and refractive index of binary aqueous ionic liquid solutions using artificial neural network. *PIChE J.*, Vol. **15**, 72-91.
47. Stoppa, A., J. Hunger, and R. Buchner (2009). Conductivities of binary mixtures of ionic liquids with polar solvents. *J. Chem. Eng. Data*, Vol. **54**, 472-479.
48. Valderrama, J.O., A. Toro, and R. E. Rojas (2011). Prediction of the heat capacity of ionic liquids using the mass connectivity index and a group contribution method.. *J. Chem.*

Thermodyn., Vol. **43**, 1068-1073.

49. Vercher, E., A. V. Orchilles, P. J. Miguel, and A. Martinez-Andreu (2007). Volumetric and ultrasonic studies of 1-ethyl-3-methylimidazolium trifluoromethanesulfonate ionic liquid with methanol, ethanol, 1-propanol, and water at several temperatures. *J. Chem. Eng. Data*, Vol. **52**, 1468-1482.
50. Viswanadhan V. N., A. K. Ghose, G. R. Revankar, and R. K. Robins (1989). Atomic physicochemical parameters for three dimensional structure directed quantitative structure-activity relationships. 4. additional parameters for hydrophobic and dispersive interactions and their application for an automated superposition of certain naturally occurring nucleoside antibiotics. *J. Chem. Inf. Comput. Sci.*, Vol. **29**, 163-172.
51. Wandschneider, A., J. K. Lehmann, and A. Heintz (2008). Surface tension and density of pure ionic liquids and some binary mixtures with 1-propanol and 1-butanol. *J. Chem. Eng. Data*, Vol. **53**, 596-599.
52. Yang, Q., H. Zhang, B. Su, Y. Yang, Q. Ren, and H. Xing (2010). Volumetric properties of binary mixtures of 1-butyl-3-methylimidazolium chloride + water or hydrophilic solvents at different temperatures. *J. Chem. Eng. Data*, Vol. **55**, 1745-1749.
53. Zafarani-Moattar, M. T. and H. Shekaari (2005a). Apparent molar volume and isentropic compressibility of ionic liquid 1-butyl-3-methylimidazolium bromide in water, ethanol, and ethanol at T = (298.15 to 318.15) K. *J. Chem. Thermodyn.*, Vol. **37**, 1029-1035.
54. Zafarani-Moattar, M. T. and H. Shekaari (2005b). Volumetric and speed of sound of ionic liquid, 1-butyl-3-methylimidazolium hexafluorophosphate with acetonitrile and methanol at *T* = (298.15 to 318.15) K. *J. Chem. Eng. Data*, Vol. **50**, 1694-1699.
55. Zafarani-Moattar, M. T. and H. Shekaari (2006a). Volumetric and compressibility behaviour of ionic liquid, 1-n-butyl-3-methylimidazolium hexafluorophosphate and tetrabutylammonium hexafluorophosphate in organic solvents at T = 298.15 K. *J. Chem. Thermodyn.*, Vol. **38**, 624-633.
56. Zafarani-Moattar, M. T. and H. Shekaari (2006b). Application of Prigogine Flory Patterson theory to excess molar volume and speed of sound of 1-n-butyl-3-methylimidazolium hexafluorophosphate or 1-n-butyl-3-methylimidazolium tetrafluoroborate in methanol and acetonitrile. *J. Chem. Thermodyn.*, Vol. **38**, 1377-1384.